**Journal of Mathematical Biology manuscript No.**
(will be inserted by the editor)

Jeff Moehlis

# Canards for a reduction of the Hodgkin-Huxley equations

the date of receipt and acceptance should be inserted later – 

**Abstract.** This paper shows that canards, which are periodic orbits for which the trajectory follows both the attracting and repelling part of a slow manifold, can exist for a two-dimensional reduction of the Hodgkin-Huxley equations. Such canards are associated with a dramatic change in the properties of the periodic orbit within a very narrow interval of a control parameter. By smoothly connecting stable and unstable manifolds in an asymptotic limit, we predict with great accuracy the parameter value at which the canards exist for this system. This illustrates the power of using singular perturbation theory to understand the dynamical properties of realistic biological systems.

## 1. Introduction: The Hodgkin-Huxley Equations

In 1952, Alan Hodgkin and Andrew Huxley published a landmark paper in the field of mathematical neuroscience [1]. Building on careful experimental observations by themselves and Bernard Katz, they presented a mathematical model for the generation of action potentials for a squid giant axon based on the dynamical interplay between ionic conductances and electrical activity. This model consists of the following equations, now referred to as the Hodgkin-Huxley equations:

$$\begin{aligned}
\frac{dV}{dt} &= [I - \bar{g}_{Na} m^3 h (V - V_{Na}) - \bar{g}_K n^4 (V - V_K) - g_L (V - V_L)]/C, \\
\frac{dn}{dt} &= \alpha_n(V)(1-n) - \beta_n(V) n, \\
\frac{dm}{dt} &= \alpha_m(V)(1-m) - \beta_m(V) m, \\
\frac{dh}{dt} &= \alpha_h(V)(1-h) - \beta_h(V) h,
\end{aligned}$$

where

$$\alpha_n(V) = \frac{0.01(V+55)}{1 - \exp[-(V+55)/10]}, \;\; \beta_n(V) = 0.125 \exp[-(V+65)/80],$$

Jeff Moehlis: Department of Mechanical and Environmental Engineering, Engineering II Building, University of California, Santa Barbara, CA 93106 U.S.A. e-mail: moehlis@engineering.ucsb.edu

**Key words:** Canards, Hodgkin-Huxley equations

$$\alpha_m(V) = \frac{0.1(V+40)}{1-\exp[-(V+40)/10]}, \;\; \beta_m(V) = 4\exp[-(V+65)/18],$$
$$\alpha_h(V) = 0.07\exp[-(V+65)/20], \;\; \beta_h(V) = \frac{1}{1+\exp[-(V+35)/10]}.$$

Here $V$ is the transmembrane potential (the voltage inside the axon minus that outside the axon), $I$ is the current injected into the neuron from a microelectrode, and $n$, $m$, and $h$ are dimensionless gating variables which each must be in the interval $[0,1]$. In these equations, voltages are measured in $mV$, current density in $\mu A/cm^2$, capacitance density in $\mu F/cm^2$, and time in $msec$. The values of the constants at $6.3°C$ are

$$\bar{g}_{Na} = 120 \; mmho/cm^2, \qquad \bar{g}_K = 36 \; mmho/cm^2, \qquad g_L = 0.3 \; mmho/cm^2,$$

$$V_{Na} = \; 50mV, \qquad V_K = -77 \; mV, \qquad V_L = -54.4 \; mV, \qquad C = 1 \; \mu F/cm^2,$$

values which will be used in the following. Note that these equations are written using modern conventions, and look slightly different from those given in [1]; one obtains the equations in this paper by letting $V_{HH} = -V - 65$. In their original paper [1], Hodgkin and Huxley showed, through numerical integration, that the dynamics of the Hodgkin-Huxley equations quite successfully matched their experimental observations. More information on mathematical issues associated with the Hodgkin-Huxley equations is given in [2,3].

The Hodgkin-Huxley equations have been hugely influential, with most serious mathematical models of the behavior of individual neurons being based on them in at least one way or another. However, as a set of four coupled, highly nonlinear ordinary differential equations, the Hodgkin-Huxley equations have proven difficult to apply detailed mathematical analysis to. More progress can be made by reducing them to a lower dimensional set of equations. We describe such a reduction in §2. The numerical bifurcation analysis of these reduced equations suggests that canards exist for this reduced system. Canards are periodic orbits for which the trajectory follows both the attracting and repelling parts of a slow manifold, and are associated with a dramatic change in properties, such as the amplitude and period, of a periodic orbit within a very narrow interval of a control parameter. In addition to their intrinsic interest, it has recently been argued that canards provide a mechanism for the synchronization of neurons at low firing frequencies in a similar set of equations [4]. In §3, we give an asymptotic analysis of the reduction of the Hodgkin-Huxley equations. Specifically, by smoothly connecting associated stable and unstable manifolds in an asymptotic limit, the parameter value at which canards exist is predicted. This prediction matches very well with the numerically obtained value. Concluding remarks, and comparisons to the full Hodgkin-Huxley equations, are given in §4.

## 2. Reduction of the Hodgkin-Huxley Equations

Here we consider a reduction of the Hodgkin-Huxley equations to a set of two coupled (but still highly nonlinear) ordinary differential equations described in [3], cf. [5]. This reduction leads to equations whose dynamics approximate the dynamics of the full Hodgkin-Huxley equations quite well, and which allow an intuitive understanding of the mathematics of action potential generation [3].

It is first noted that the equations for the gating variables $n, m$, and $h$ can be written in the form

$$\tau_j(V)\frac{dj}{dt} = j_\infty(V) - j, \tag{1}$$

where

$$j_\infty(V) \equiv \frac{\alpha_j(V)}{\alpha_j(V)+\beta_j(V)}, \qquad \tau_j(V) \equiv \frac{1}{\alpha_j(V)+\beta_j(V)}, \tag{2}$$

with $j \in \{n, m, h\}$. It is found that the time constant $\tau_m$ is much smaller than $\tau_n$ and $\tau_h$ over the entire relevant range of $V$. Thus, $m$ evolves faster than $n$ or $h$. This suggests that we replace $m(t)$ in the Hodgkin-Huxley equations by $m_\infty(V(t))$, an approximation shown to be reasonable through numerical simulations.

Next, it is observed numerically that when the solutions to the Hodgkin-Huxley equations correspond to periodic action potentials, the following equation approximately holds:

$$n(t) + h(t) \approx 0.8. \tag{3}$$

Note that Equation (3) should be viewed as an observation - it has no rigorous mathematical or biological basis. We choose to eliminate the gating variable $h$ by taking $h(t) = 0.8 - n(t)$.

With these simplifications, we obtain the following two-dimensional system of equations:

$$\frac{dV}{dt} = \{I - \bar{g}_{Na}[m_\infty(V)]^3(0.8-n)(V-V_{Na}) - \bar{g}_K n^4(V-V_K) - g_L(V-V_L)\}/C, \tag{4}$$

$$\frac{dn}{dt} = \alpha_n(V)(1-n) - \beta_n(V)n. \tag{5}$$

Figure 1 shows a bifurcation diagram for equations (4) and (5) with $I$ treated as the bifurcation parameter; this was calculated using AUTO97 [6]. It is found that a stable fixed point (with $V_{max} - V_{min} = 0$, corresponding to a steady voltage and the absence of action potentials) exists for small values of $I$. This loses stability in a subcritical Hopf bifurcation as $I$ increases through $I = 8.82$. The resulting branch of periodic orbits bifurcates to smaller values of $I$, and undergoes a saddlenode bifurcation at $I = 6.36$, leading to a stable periodic orbit corresponding to stable, periodically firing action potentials;

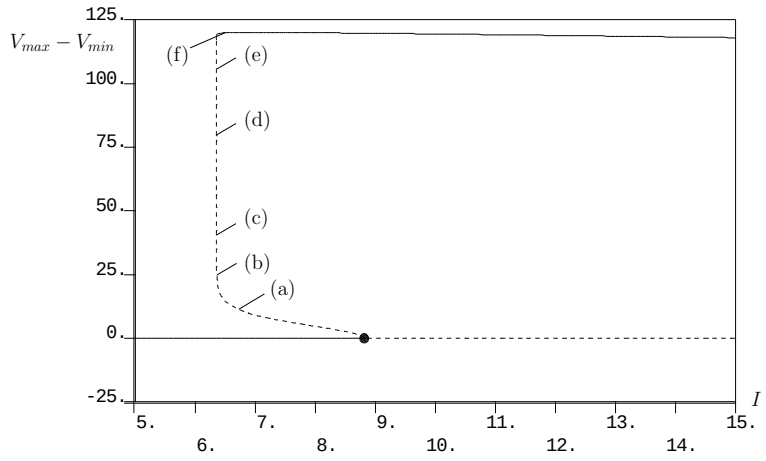


**Fig. 1.** Bifurcation diagram for equations (4) and (5). Solid and dashed lines correspond to stable and unstable solutions, respectively. The letters refer to the phase space plots shown in Figure 2.

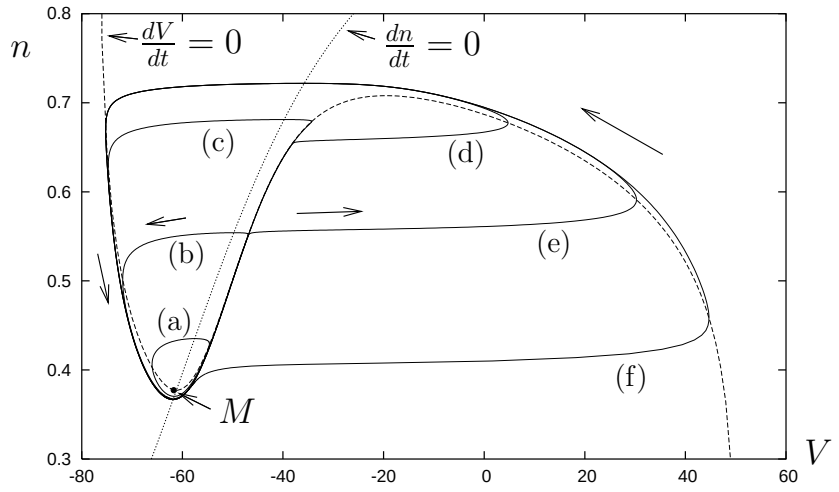


**Fig. 2.** Projection of periodic orbits at points on the branch indicated in Figure 1. The dashed (resp., dotted) line shows the $V$-nullcline (resp., $n$-nullcline). The point labelled $M$ is at the local minimum of the $V$-nullcline.

see Figure 2 for phase space projections of these periodic orbits, and Figure 3 for a timeseries for $V$ for the stable periodic orbit at $I = 6.5$. Both the fixed point and a periodic orbit are stable for $6.36 \leq I \leq 8.82$.

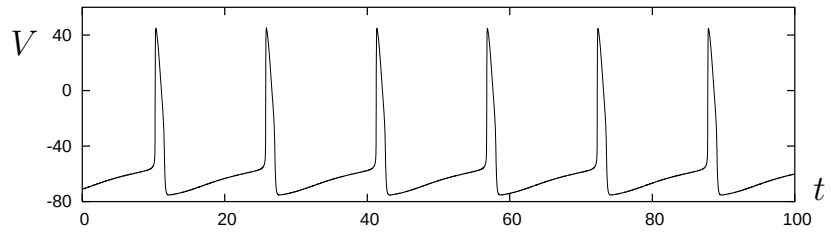


**Fig. 3.** Time series for the stable periodic orbit at $I = 6.5$, indicated as (f) on Figures 1 and 2.

We find that the periodic orbit along this branch changes its properties very dramatically in a very narrow interval of the bifurcation parameter $I$. This, and the fact that the periodic orbits in Figure 2 "hug" the "middle" part of the $V$-nullcline, suggests that the periodic orbits near $I = 6.36$ are canards, i.e., periodic orbits for which the trajectory following both the attracting and the repelling parts of a slow manifold. Canards were first found in a study of the van der Pol system using techniques from nonstandard analysis [7,8], and have since been studied for a variety of chemical, biological, and other systems; see, e.g., [9–16] and other references in [17]. In particular, see [10,11,13] for studies of canards for the FitzHugh-Nagumo equations, which can be viewed as idealizations of equations (4) and (5) obtained by assuming that the $V$-nullcline is cubic and that the $n$-nullcline is linear. In the next section, we will predict the value of $I$ at which the canards (and the associated saddlenode bifurcation) occur for equations (4) and (5), using singular perturbation techniques and help from Mathematica.

## 3. Analysis of Canards for the Reduced Equations

When equations (4) and (5) exhibit periodically firing action potentials, it can be verified numerically that

$$\left|\frac{dV}{dt}\right| \gg \left|\frac{dn}{dt}\right|. \tag{6}$$

Therefore, the dynamics of $V$ are much faster than the dynamics of $n$. We call $V$ a fast variable and $n$ a slow variable. This suggests that it might be possible to understand the dynamics of this system using techniques from singular perturbation theory. We rewrite equations (4) and (5) as

$$\frac{dV}{dt} = f(V, n; I), \tag{7}$$

$$\frac{dn}{dt} = \epsilon g(V, n), \tag{8}$$

where

$$f(V,n;I) = \{I - \bar{g}_{Na}[m_\infty(V)]^3(0.8-n)(V-V_{Na}) \\ -\bar{g}_K n^4(V-V_K) - g_L(V-V_L)\}/C, \tag{9}$$

$$g(V,n) = \alpha_n(V)(1-n) - \beta_n(V)n. \tag{10}$$

Here we are using a common trick in asymptotic analysis, namely we will treat $\epsilon$ as a small parameter when doing expansions, but in our final formulas will plug in $\epsilon = 1$; see, e.g., [18].

If $\epsilon$ is set equal to zero, then the $V$-nullcline is a curve of fixed points. This curve is normally hyperbolic on the pieces for which its slope is bounded away from zero, i.e., away from the local minimum $M$ and local maximum of the $V$-nullcline in Figure 2. For $\epsilon = 0$, the "left" and "right" parts of the $V$-nullcline are found to be stable to transverse perturbations, while the "middle" part is found to be unstable to transverse perturbations.

Invariant manifold theorems then imply that for $\epsilon$ sufficiently small, invariant manifolds persist within $O(\epsilon)$ of these normally hyperbolic pieces of the $V$-nullcline, with the manifolds inheriting their normal stability properties from the stability properties of the pieces of the $V$-nullcline [19–21]. There will thus be a slow manifold $M_S$, with stable foliation, within $O(\epsilon)$ of the "left" part of the $V$-nullcline, a different slow manifold, with stable foliation, within $O(\epsilon)$ of the "right" part of the $V$-nullcline, and a slow manifold $M_U$, with unstable foliation, within $O(\epsilon)$ of the "middle" part of the $V$-nullcline. The manifolds $M_S$ and $M_U$ can be extended beyond the point $M$ according to the flow, but the extensions may leave an $O(\epsilon)$ distance of the $V$-nullcline, and may also lose their normal stability properties.

Generically, the distance between $M_S$ and $M_U$ is nonzero near $M$. Sketches of the relative positions of these invariant manifolds near $M$ are shown in Figure 4 for different parameter ranges; these sketches also include fixed points and/or periodic orbits which must be present for this system. The distance between $M_S$ and $M_U$ near $M$ changes as parameters are varied, and it is possible for particular parameters that the manifolds $M_S$ and $M_U$ will connect smoothly. Following [12], the resulting invariant curve is called a *canard manifold*. In this situation, nearby trajectories follow the canard manifold both along its attracting and repelling parts. Using asymptotic expansions, we will approximate the value for $I$ at which canards exist by requiring the existence of a canard manifold which stays within $O(\epsilon)$ of the $V$-nullcline. This procedure closely follows that given in [12] and [17].

We begin by noting that trajectories for equations (7) and (8) must satisfy

$$f(V,n;I)\frac{dn}{dV} = \epsilon g(V,n). \tag{11}$$

We now expand

$$I = I_0 + \epsilon I_1 + \cdots \tag{12}$$

$$n = n(V;I) = n_0(V;I_0) + \epsilon n_1(V;I_0,I_1) + \cdots \tag{13}$$

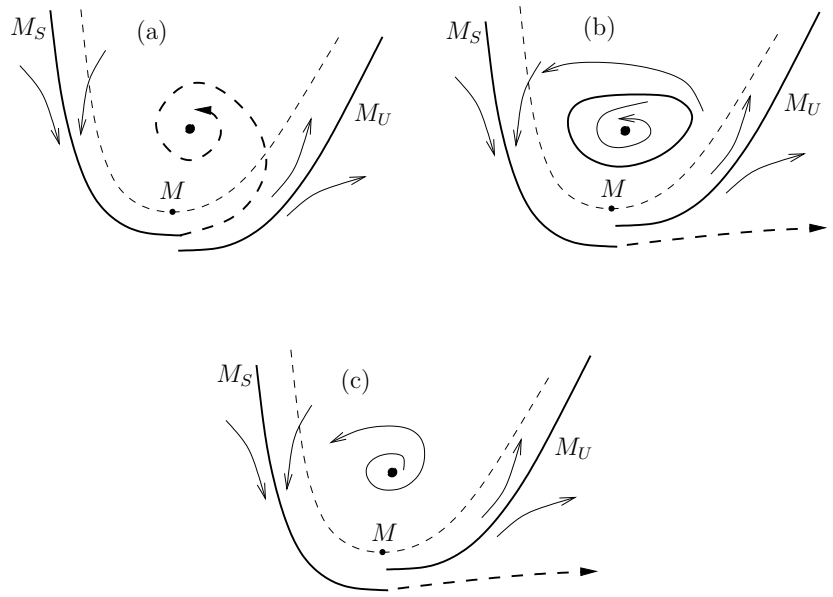


**Fig. 4.** Sketch of the relative positions of the stable and unstable manifolds near $M$ for $\epsilon > 0$. The $V$-nullcline is shown as a thin dashed line. The trajectory follows the stable manifold $M_S$, and after passing near $M$ may either (a) cross the $V$-nullcline and tend toward the stable fixed point, or (b,c) undergo a large excursion before returning to a neighborhood of $M_S$, giving a large relaxation-oscillation periodic orbit. In (b), there is also an unstable small periodic orbit which surrounds a stable fixed point. The sketches for (a), (b), and (c) are appropriate for equations (4) and (5) with $I < 6.36$, $6.36 < I < 8.82$, and $I > 8.82$, respectively.

$$f(V, n; I) = f_0(V, n_0; I_0) + \epsilon f_1(V, n_0, n_1; I_0, I_1) + \cdots \tag{14}$$

$$g(V, n) = g_0(V, n_0) + \epsilon g_1(V, n_1) + \cdots. \tag{15}$$

The curve $n(V; I)$ will be our approximation to the canard manifold.

At $O(\epsilon^0)$, equation (11) becomes

$$f_0 \frac{dn_0}{dV} = 0. \tag{16}$$

In order for $n_0$ to be nontrivial, this requires that $f_0 = 0$. This implies that

$$I_0 - \bar{g}_{Na}[m_\infty(V)]^3(0.8 - n_0)(V - V_{Na}) - \bar{g}_K n_0^4(V - V_K) - g_L(V - V_L) = 0, \tag{17}$$

a quartic equation that can be solved symbolically using Mathematica to give $n_0(V; I_0)$. The resulting equation is too long to be given here. (Actually, there are four possible solutions; the appropriate one lies in the biologically relevant part of phase space.)

At $O(\epsilon)$, using the fact that $f_0 = 0$, equation (11) becomes

$$f_1 \frac{dn_0}{dV} = g_0, \tag{18}$$

which can be rearranged to give

$$f_1 = \frac{g_0}{dn_0/dV}, \tag{19}$$

where

$$g_0 = \alpha_n(V)(1-n_0) - \beta_n(V)n_0. \tag{20}$$

In order to keep $f_1$ bounded (as required for the asymptotic expansion to be valid) we need $g_0$ to vanish at the value for $V$ at which $dn_0/dV = 0$. This gives a set of two algebraic equations which can be solved for $I_0$ and $V$, and which are equivalent to choosing $I_0$ such that the $n$-nullcline intersects the $V$-nullcline at its local minimum, cf. [12,17]. Solving these numerically with Mathematica, we find

$$I_0 = 6.52, \qquad V = -61.12.$$

Using this value for $I_0$ and the appropriate solution to (17), equation (19) gives an (analytical) formula for $f_1$. We do not give the formula here because of its length.

Of course, $f_1$ can also be obtained by direct expansion of $f(V,n;I)$. We obtain

$$f_1 = \{I_1 + \bar{g}_{Na}[m_\infty(V)]^3 n_1(V-V_{Na}) - 4\bar{g}_K n_0^3 n_1(V-V_K)\}/C. \tag{21}$$

Equating (19) and (21), we obtain the following equation for $n_1$:

$$n_1 = \frac{Cg_0/\frac{dn_0}{dV} - I_1}{\bar{g}_{Na}[m_\infty(V)]^3(V-V_{Na}) - 4\bar{g}_K n_0^3(V-V_K)}. \tag{22}$$

At $O(\epsilon^2)$, again using the fact that $f_0 = 0$, equation (11) becomes

$$f_1\frac{dn_1}{dV} + f_2\frac{dn_0}{dV} = g_1, \tag{23}$$

where

$$g_1 = -\alpha_n(V)n_1 - \beta_n(V)n_1. \tag{24}$$

This can be rearranged to give

$$f_2 = \frac{g_1 - f_1 dn_1/dV}{dn_0/dV}. \tag{25}$$

In order to keep $f_2$ bounded (as required for the asymptotic expansion to be valid) we need the numerator $p \equiv g_1 - f_1 dn_1/dV$ to vanish at the value for $V$ at which $dn_0/dV = 0$, namely $V = -61.12$ as determined above. This gives an algebraic equation for $I_1$. However, it is found that it is difficult to accurately calculate $p$ with Mathematica near this value for $V$: $g_0$ and $dn_0/dV$ tend to zero here, and both $f_1$ (see (19)) and $g_1$ (see (24) and (22)) depend on the ratio of these quantities. We thus find $I_1$ by setting $p$ equal to zero for nearby values of $V$, and fitting a quadratic function to obtain the value of $I_1$ at $V = -61.12$; see Figure 5. This gives

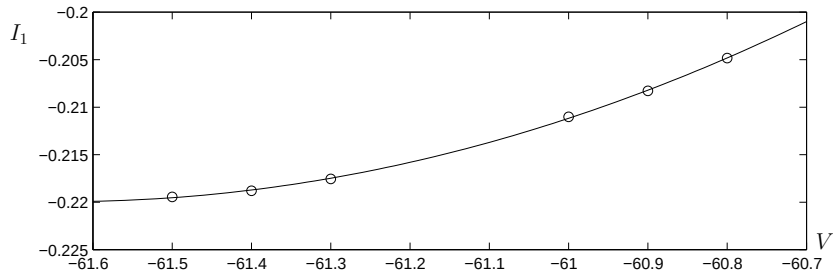


**Fig. 5.** The dots show the values of $I_1$ for which the function $g_1 - f_1 dn_1/dV$ vanishes for different values for $V$, and the line shows the quadratic fit which allows us to determine the value of $I_1$ for which the function vanishes when $V = -61.12$.

$I_1 = -0.21$. (Alternatively, one could use L'Hospital's rule to evaluate the limit of $g_0/(dn_0/dV)$ for use in (19) and (22), as done for example in a similar calculation in [17].) Thus, the value for $I$ at which the canard manifold exists, to this order, is

$$I = I_0 + \epsilon I_1 + \cdots \approx 6.52 + (1)(-0.21) = 6.31. \tag{26}$$

This matches quite favorably with the numerically obtained value of $I = 6.36$ at which canards are found for equations (4) and (5). We do not attempt here to continue of asymptotic analysis to higher order in $\epsilon$.

## 4. Conclusion

We have shown numerically that canards, i.e., periodic orbits for which the trajectory follows both the attracting and repelling part of a slow manifold, can exist for a two-dimensional reduction of the Hodgkin-Huxley equations described in [3]. Such canards are associated with a dramatic change in properties, such as the amplitude and period, of the periodic orbit within a very narrow interval of a control parameter. By smoothly connecting stable and unstable manifolds in an asymptotic limit, we predicted with great accuracy the parameter value at which the canards exist for this system. This analysis illustrates the power of using singular perturbation theory to understand the dynamical properties of realistic biological systems. Indeed, similar techniques can be used to predict parameter values at which canards and/or bifurcations exist for many systems of biological and physical interest; see, e.g., [11,12,18,17]. The canards identified in this paper are loosely related to those described in [4] for a similar set of equations which includes an additional slow synaptic variable; that paper argues that canards can provide a mechanism for the synchronization of neurons at low firing frequencies.

The basic bifurcation behavior for the reduced equations considered here is that a fixed point loses stability in a subcritical Hopf bifurcation, with a "small" unstable periodic orbit bifurcating to lower values of $I$. As the

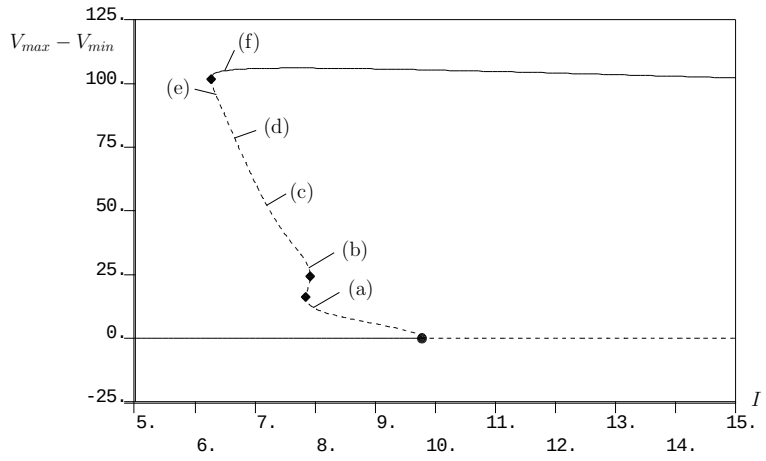


**Fig. 6.** Bifurcation diagram for the Hodgkin-Huxley equations. Solid and dashed lines correspond to stable and unstable solutions, respectively. The circle and diamonds indicate the locations of Hopf and saddlenode bifurcations, respectively. The letters refer to the phase space plots shown in Figure 7.

periodic orbit branch is followed, it reaches a value for $I$ at which the periodic orbit rapidly changes to a "large" periodic orbit by passing through canards. At almost exactly the same parameter value at which the canards exist, there is a saddlenode bifurcation of the periodic orbits, so that as the branch is followed beyond this bifurcation there is a stable, "large" periodic orbit. This is typical behavior for systems undergoing a singular subcritical Hopf bifurcation [10].

It is natural to ask if this bifurcation and canard behavior is present in the full Hodgkin-Huxley equations. See Figure 6 for the bifurcation diagram with $I$ treated as the bifurcation parameter, computed using AUTO97 [6]; this is consistent with results from [22]. The vertical axis shows $V_{max} - V_{min}$ for the solutions, and stable (resp. unstable) solutions are indicated by solid (resp. dashed) lines. A stable fixed point (with $V_{max} - V_{min} = 0$, corresponding to a steady voltage and the absence of action potentials) exists for small values of $I$. This loses stability in a subcritical Hopf bifurcation as $I$ increases through $I = 9.78$. The resulting branch of periodic orbits bifurcates to smaller values of $I$, and undergoes saddlenode bifurcations at $I = 7.85$, $I = 7.92$, and $I = 6.26$, the last of which leads to stable periodic orbits corresponding to stable, periodically firing action potentials; see Figure 7 for phase space projections of these periodic orbits. Both the fixed point and a periodic orbit are stable for $6.26 \leq I \leq 9.78$.

Comparing Figures 1 and 6, and 2 and 7, we see that there are certainly similarities between the bifurcation and dynamical behavior for the full Hodgkin-Huxley equations and the reduced equations. However, the transi-

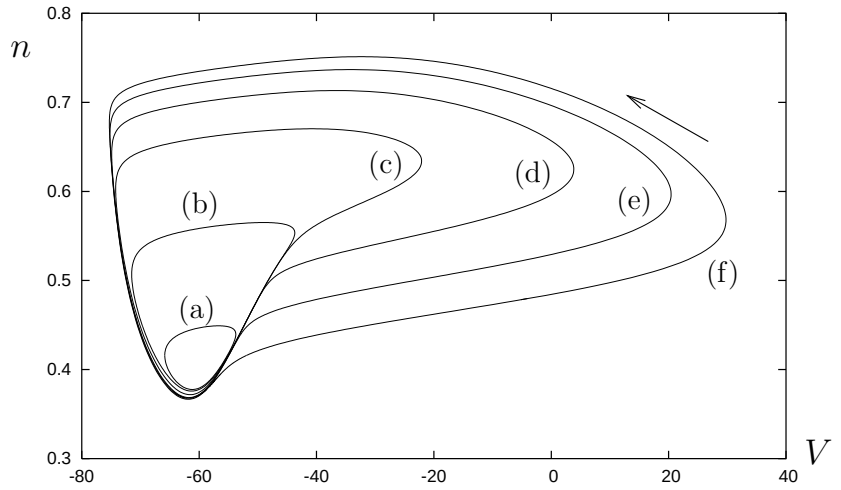


**Fig. 7.** Projection of periodic orbits at points on the branch indicated in Figure 6.

tion from "small" to "large" periodic orbits occurs over a much larger range of values for $I$ for the full Hodgkin-Huxley equations. This discrepency leads us to re-examine the assumptions leading to equations (4) and (5). The first assumption was that $m$ could be replaced by $m_\infty(V)$; Figure 8, which compares these quantities for two periodic orbits from Figure 6 and 7, shows that this is reasonable. The second assumption, that $n + h = 0.8$, is more suspect, as seen in Figure 9. Other linear relationships between $n$ and $h$ have been proposed, such as $5n/4 + h = 1$; using this to eliminate $h$ as in the derivation of (4) and (5) gives reduced equations with a similar bifurcation diagram, but with the canards and associated saddlenode bifurcation occurring at $I = 3.36$. Using the better approximation of $5n/4 + h = 0.9$ (see Figure 10) gives canards and the associated saddlenode bifurcation at $I = 6.14$, to be compared with the value of $I = 6.26$ for the saddlenode bifurcation of periodic orbits for the full Hodgkin-Huxley equations. This is of comparable accuracy to the result the saddlenode bifurcation of periodic orbits for the approximate equations (4) and (5) occurs at $I = 6.36$.

A study of the appropriate nullcline surfaces and stable and unstable manifolds, perhaps with the assumption that $m$ can be replaced by $m_\infty$, might help to clarify the relevance of canards for the full Hodgkin-Huxley equations.

## References

1. Hodgkin, A. L., Huxley, A. F.: A quantitative description of membrane current and its application to conduction and excitation in nerve. *J. Physiol.* **117**, pp. 500-544 (1952)
2. Cronin, J.: Matematical Aspects of Hodgkin-Huxley neural theory. Cambridge: Cambridge University Press, 1987

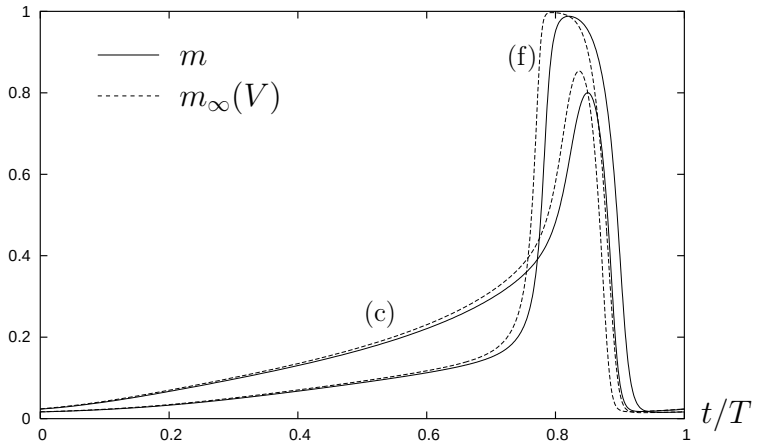


**Fig. 8.** Comparison of $m$ (solid lines) and $m_\infty(V)$ (dashed lines) for the periodic orbits labelled (c) and (f) in Figures 6 and 7. The horizontal axis shows $t$ normalized by the period $T$ of the appropriate periodic orbit.

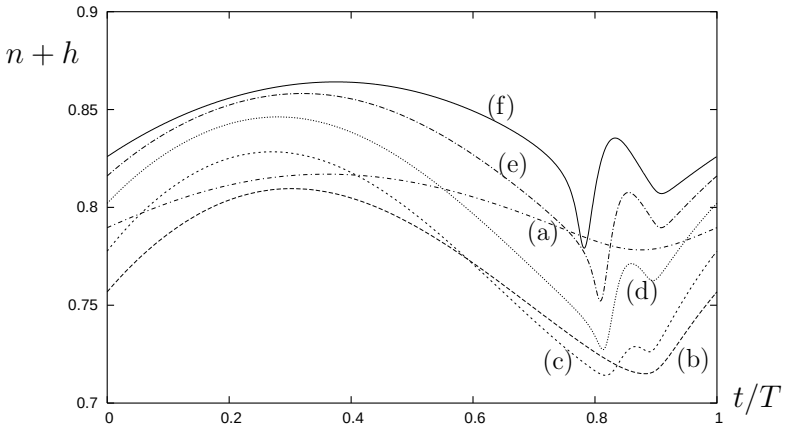


**Fig. 9.** Values for $n+h$ for the periodic orbits in Figures 6 and 7. The horizontal axis shows $t$ normalized by the period $T$ of the appropriate periodic orbit.

3. Keener, J., Sneyd, J.: Mathematical Physiology. New York: Springer, 1998
4. Drover, J., Rubin, J., Su, J., and Ermentrout, B.: Analysis of a canard mechanism by which excitatory synaptic coupling can synchronize neurons at low firing frequencies. Preprint.
5. Rinzel, J.: Excitation dynamics: insights from simplified membrane models. *Federation Proc.* **44**, pp. 2944–2946 (1985)
6. Doedel, E., Champneys, A., Fairgrieve, T., Kuznetsov, Y., Sandstede, B., Wang X.: AUTO 97: Continuation and bifurcation software for ordinary differential equations. Available via FTP from directory /pub/doedel/auto at ftp.cs.concordia.ca, 1997

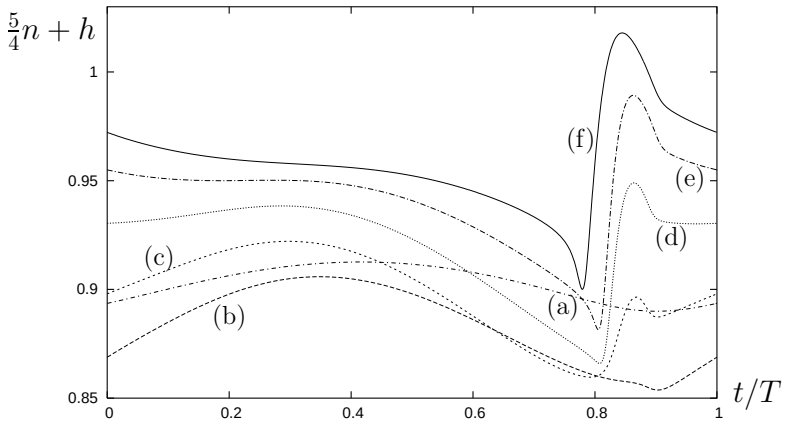


**Fig. 10.** Values for $5n/4 + h$ for the periodic orbits in Figures 6 and 7. The horizontal axis shows $t$ normalized by the period $T$ of the appropriate periodic orbit.


7. Callot, J.-L., Diener, F., Diener, M.: Le problème de la "chasse au canard". *C. R. Acad. Sci. Paris (Sér. I)* **286**, pp. 1059–1061 (1978)
8. Benoit, E., Callot, J.-L., Diener, F., Diener, M.: Chasse au canard. *Collect. Math.* **32**, pp. 37–119 (1981)
9. Eckhaus, W.: Relaxation oscillations including a standard chase on French ducks. *Lecture Notes in Math.* **985**, pp. 449–494 (1983)
10. Baer S. M., Erneux, T.: Singular Hopf bifurcation to relaxation oscillations. *SIAM J. Appl. Math.* **46**, pp. 721–739 (1986)
11. Brøns, M.: Excitation and annihilation in the FitzHugh-Nagumo equations. *IMACS Trans. Sci. Comp.*. **1.1**, pp. 297–301 (1989)
12. Brøns, M., Bar-Eli, K.: Canard explosion and excitation in a model of the Belousov-Zhabotinsky reaction. *J. Phys. Chem.* **95**, pp. 8706–8713 (1991)
13. Baer, S. M., Erneux, T.: Singular Hopf bifurcation to relaxation oscillations II. *SIAM J. Appl. Math.* **52**, pp. 1651–1664 (1992)
14. Guckenheimer, J., Hoffman, K., Weckesser, W.: Numerical computation of canards. *Int. J. Bif. Chaos* **10**, pp. 2669–2687 (2000)
15. Krupa, M. Szmolyan, P.: Relaxation oscillation and canard explosion. *J. Diff. Eq.* **174**, pp. 312–368 (2001)
16. Szmolyan, P. Wechselberger, M.: Canards in $R^3$. *J. Diff. Eq.* **177**, pp. 419–453 (2001)
17. Moehlis, J.: Canards in a surface oxidation reaction. *J. Nonlin. Sci.* **12**, pp. 319–345 (2002)
18. Brøns, M., Bar-Eli, K.: Asymptotic analysis of canards in the EOE equations and the role of the inflection line. *Proc. R. Soc. Lond. A* **445**, pp. 305–322 (1994)
19. Fenichel, N.: Persistence and smoothness of invariant manifolds for flows. *Indiana Univ. Math. Journal* **21** pp. 193–226 (1971)
20. Fenichel, N.: Geometric singular perturbation theory for ordinary differential equations. *J. Diff. Eq.* **31**, pp. 53–98 (1979)
21. Wiggins, S.: Normally Hyperbolic Invariant Manifolds in Dynamical Systems. New York: Springer, 1994
22. Rinzel, J., Miller, R. N.: Numerical calculations of stable and unstable periodic solutions to the Hodgkin-Huxley equations. *Math. Biosci.* **49**, pp. 27-59 (1980)